



# Comparison Study between Theoretical and Numerical Analyses for Ball Bearing

**Badr H. Bedairi<sup>1</sup>, Ahmed B. Khoshaim<sup>2</sup> and Badr S. Azzam<sup>1\*</sup>**

<sup>1</sup>College of Engineering, Taibah University, Madinah Al Munawara, KSA.

<sup>2</sup>College of Engineering, King Abdul-Aziz University, Jeddah, KSA.

## **Authors' contributions**

*This work was carried out in collaboration among all authors. All authors read and approved the final manuscript.*

## **Article Information**

DOI: 10.9734/JERR/2021/v20i1117402

### Editor(s):

(1) Prof. Hamdy Mohy El-Din Afefy, Tanta University, Egypt.

### Reviewers:

(1) Marwa Mohamed El-Sayed, National Research Centre, Egypt.

(2) Yuhou Wu, Shenyang Jianzhu University, China.

Complete Peer review History: <https://www.sdiarticle4.com/review-history/71436>

**Case Studies**

**Received 18 May 2021**  
**Accepted 28 July 2021**  
**Published 31 July 2021**

## **ABSTRACT**

In this paper, a comparison study has been presented to see the difference between the theoretical and finite element analysis for ball bearing. Throughout that study, a finite element analysis is performed to determine the maximum contact pressure and maximum stresses induced in the bearing components; rolling elements and rings. Another purpose of this analysis is to validate the most critical zones in the bearing for knowing the scenario of generating this stress and pressure which enabling the specialists to determine the initiation point for failure in the bearing. The comparison between the results of the numerical study with theoretical one has showed the good agreement outputs of this numerical study. In addition, this analysis could give the displacements and deformations that raised in the bearing elements at the highest critical zones.

**Keywords:** *Rolling bearings; finite element analysis; stress analysis; failure mechanics; ABACOS and numerical analysis.*

## **1. INTRODUCTION**

Rolling bearings are mechanical elements used in machines to support any rotating members

(shafts, rotors, impellers, etc.) in order to reduce the friction and wear of these parts. Where, the friction may cause more power losses of machines which lead to a decrease in their

\*Corresponding author: Email: [badr\\_azzam@yahoo.com](mailto:badr_azzam@yahoo.com);

efficiency. Reducing the friction can also decrease the wear of these parts and so keeping the fits between these parts as designed and making the vibration in its allowable ranges.

Rolling bearings are different than sliding bearings in various aspects such as: speed, life, lubrication, loading, mounting fits and failure phenomenon. One of the most important notices of rolling bearings is its failure, where they give some performance signals before going to failure as; noise, vibration, heat, or leak. Generally, there are many causes for rolling bearing failures. Some of these causes are related to overloading the bearings, some are related to the mounting processes and the others are related to the environmental conditions. The bearing failure may be in the rolling elements, inner ring, outer ring or the cage. Therefore, it is very important for the bearing designer to determine the position of the critical element in the bearing, which may be much affected by these causes. This will enable the people work in that area to analyze the failure in the bearing under different working conditions and so performing the reasonable maintenance. For the stress analysis of rolling bearings, the contact pressure between the different contact elements of bearings is obtained using the Hertz theory [1].

This theory can determine the stress and deformation at the most critical contact areas of the ball bearings at two different zones. The first zone is between the ball and inner ring, whereas the other zone is between the ball and the outer ring.

In order to get the stress distribution at these two zones, a FEA study has been done by Mootoka et al. [2] to solve the contact problem of the roller bearings. They have built an approximate contact model using a roller contacting a surface of infinite length. Throughout, that analysis, Mootoka and his colleagues have suggested a numerical model to do the contact analysis of the roller bearings. They have used the FEM module in SolidWorks and some other finite element methods to get the maximum contact pressure and radial contact rigidity of the ball bearing with referring to Hertz theory. They have found that the results obtained by the special software are nearly similar to the results obtained by Hertz theory.

Viramgama [3] has manipulated in his paper the analysis of single row deep groove ball bearing. He performed static and dynamic analyses for

that bearing. The main conclusion of his work was that the deformation of that bearing in static condition was less than that of dynamic condition and the maximum stress was less than that in the dynamic conditions. Finally, he could conclude that his bearing is safe against the radial and axial load, which is applied at static and dynamic condition.

Peter et al. [4] have presented a study showing the comparison between analytical and numerical solution of bearing contact analysis. In their study, they analyzed the rolling ball bearing using finite element analysis to see the contact pressure level and the stress or displacement behavior of rolling ball bearing. They compared between their results with the analytical results obtained through the methodology of Hertz theory. The comparison showed a reasonable composition and solution of analytical formulas and equations based on specific ball bearing parameters were obtained to achieve optimal results. Additionally, an almost identical similarity of results of numerical and analytical solution is correct setting up of the given simulation in computational software ANSYS.

Belabend et al. [5] have performed a theoretical and numerical analysis for deep groove ball bearings based on static loadings. The purpose of their study was to collect data's using two different softwares and then compared them with analytical results. That work aimed to analyze the behavior of the ball bearings under static loads, using Solidworks, ANSYS and MESYS software. The comparison was done between the finite element results and the analytical results using the Hertzian theory for two different cases of loading. The maximum stress was found to be at the lower ring raceway (i.e. between the ball and inner ring) with  $P_{max} = 946$  MPa which agree well with the theoretical results by an approximate deviation of 2 %. The failure in the rolling element bearings was found to be as fatigue wear type due to the high contact pressure at the ball surface.

## **2. THEORETICAL ANALYSIS FOR BALL BEARINGS**

### **A- Number of Loaded Balls in the Bearing and the Equivalent Load**

Generally, the reactions of bearing due to the applied loads are transmitted to its housing via the bearing elements. The equivalent load of these reactions is not simultaneously sustained

by all balls in bearing. It is distributed on a certain number of balls in the bearing. The number of loaded balls is determined from the following equation, as shown in Fig. (1) [6]:

$$Z_s = 2 \text{INT} \left( \frac{Z+3}{4} \right) - 1 \quad (1)$$

$$n = \frac{Z_s - 1}{2} \quad (2)$$

Where;

Z : total number of balls in the bearing.

Z<sub>s</sub>: number of balls sustaining the applied loads.

n : number of loaded balls in one side of the bearing from the vertical axis.

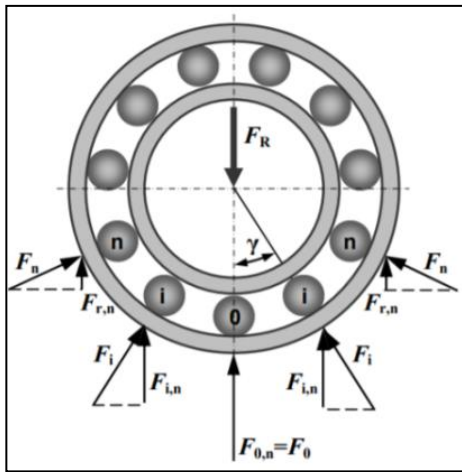


Fig. 1. Distribution of loads in the ball bearing [6]

### B- Contact (Hertzian) Stresses in the Bearing Elements

The contact analysis presented by Heinrich Hertz was based on the following assumptions [4]:

- 1- The contact surfaces are continuous, smooth, nonconforming, and frictionless,
- 2- The contact area is very small compared to the size of the two bodies,
- 3- In the vicinity of the contact zone, the behavior of the solid contact bodies can be considered elastic half-space.

The Hertzian contact pressure distribution within the contact area between the balls and the two rings at the contact zones will be of hemispherical shape with a maximum value  $P_{max}$  at the center point of the contact area [6], as shown in Fig. (2).

$$P_{max} = \frac{3F}{2\pi a^2} \quad (3)$$

Where;

The contact area radius "a" can be determined from the following equation [7]:

$$a = \sqrt[3]{\frac{3F}{8} \left[ \frac{(1-\nu_1^2)/E_1 + (1-\nu_2^2)/E_2}{1/d_1 + 1/d_2} \right]} \quad (4)$$

Where;

d<sub>1</sub> and d<sub>2</sub> : diameters of the ball and ring recesses (inner or outer), shown in Fig. (2). (d<sub>2</sub> is taken with negative value).

E<sub>1</sub> and E<sub>2</sub>: elasticity modules of the ball and ring materials, respectively.

ν<sub>1</sub> and ν<sub>2</sub> : Poisson's ratio of the ball and ring materials, respectively.

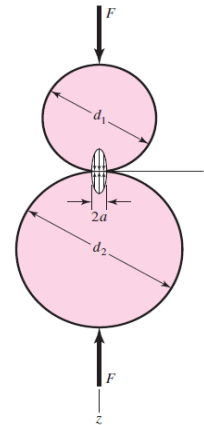


Fig. 2. Contact pressure distribution between two spherical bodies [7]

### 3. NUMERICAL ANALYSIS FOR BALL BEARINGS

The numerical analysis has been conducted using ABAQUS standard FE software. The Hertzian contact problem has been validated in section 1.1.11 of the user manual [8]. Therefore, the investigated bearing was simulated and solved through two models; linear model and quadratic model, with given material properties of linear elastic and modulus of elasticity.

Due to the symmetric nature of the problem, only 2D axisymmetric was conducted to simulate the maximum contact pressure and the maximum von-Mises stresses and its distance.

The element types used were CAX4 and CAX8: a 4 and 8-node bi-quadratic axisymmetric quadrilateral. The boundary conditions were made so that the force and the corresponding displacement follow the reasonable movements of the contacting mates (e.g. rings and the ball). Therefore, the flat surface of the outer ring was fixed in the x-axis as XSYMM ( $U1=UR2=UR3=0$ ), as shown in Fig. 3. The outer ring top surface was fixed in all rotation and translation degrees of freedom (ENCASTERE). A reference point at the center of the bearing created to be used as a guide to the applied force.

The reference point at the center of the ball bearing was coupled with the inner ring outer surface. The coupling type was Kinematic constraining all DOF. The reference point was constrained in all rotation and translation except in y-axis ( $U2$ ) to maintain the direction of the applied forces on the balls, as given in Fig. 3.

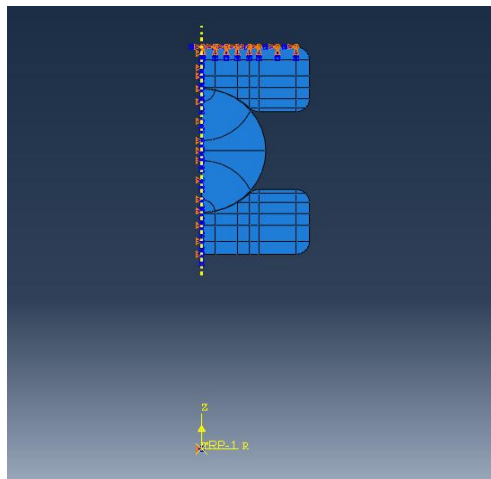


**Fig. 3. The boundary conditions of the ball bearing under investigation**

The first contact pair was selected as the upper half ball as the slave and the outer ring race way as the master. Whereas the second contact pair was selected as the lower half of the ball as the slave and the inner ring raceway as the master.

The contact properties were selected as tangential behavior and normal behavior. The tangential behavior was considered for the penalty for the friction formulation with friction coefficient equals to 0.2. Whereas the normal behavior was considered for the hard contact option for the pressure-overclosure and default constraint enforcement method. The contact pairs are shown in

Fig. 4. The analysis steps have been run as linear analysis.

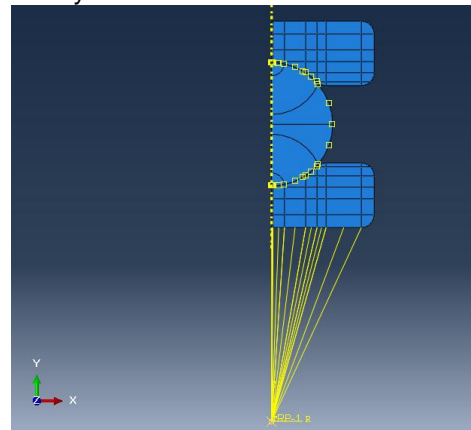


**Fig. 4. Contact pairs of the bearing under investigation**

#### 4. CASE STUDY

In this case study analysis, a rolling bearing of number 6206-SKF has been used for that numerical analysis. The data of that bearing are shown below, see Fig. (5) [9]:

- Bore diameter of bearing ( $d$ )= 30 mm
- Outer diameter of bearings ( $D$ )= 62 mm
- Pitch diameter ( $D_p$ )= 46 mm
- Ball diameter ( $d_b$ )= 9.525 mm
- Raceway diameter of outer ring= 55.525 mm
- Raceway diameter of inner ring= 36.475 mm
- Face width ( $B$ )= 16 mm
- Number of balls= 9 balls
- Outer ring and inner ring recess radii ( $r_2$ )= 5 mm.
- Dynamic capacity ( $C$ )= 20.3 kN
- Static capacity ( $C_0$ )= 11.2 kN

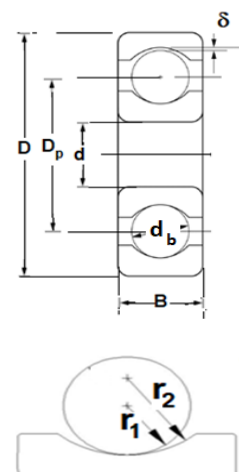


**Fig. 5. Bearing dimensions**

### 4.1 Loading Data

The applied radial load is taken as 10 kN (with no axial load) as taken by Bedairi et al. [8]. As mentioned in that paper, that the load will not be equally distributed among the loaded balls. The angle spacing the balls was 40°. The number of balls that sustained the applied load was 5 balls (from equation 2) and the number of loaded balls on one side of the vertical axis was 2 (from equation 3). The maximum radial load will be on the central ball with a value of 3.47 kN. The applied force on the reference point was F equals to 1.735 kN, which is half of the full model force over the critical ball.

stresses and deformations raised in the different parts of the ball bearing. This numerical analysis has focused on the study of the effect of load in two zones, which contain the critical regions in the bearing. The first critical region is the contact area zone-1, which is between the lower half ball and the inner ring raceway, whereas the other region is the contact zone-2 which is between the upper half ball and the outer ring raceway. The materials of the rings and rolling elements in that bearing is carbon chromium steel with mechanical properties as given in Table (1) [11]. The number of elements and element type has been also shown in that table. The element mesh at the two contact zones between the ball and rings are shown in Figs. 6 and 7.

## 5. ANALYSIS RESULTS

### A- Theoretical Results

According to Bedairi et al. [10], the maximum contact pressure obtained, using equations 3 and 4, was found to be 962 MPa at the mid-point of the contact area. Whereas the maximum von-Mises stress between the ball and rings was 596 MPa. The bearing deformation due to the applied load could be determined and found to be as 0.105 mm (refer to reference 10).

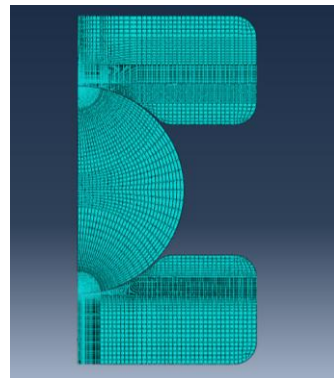


Fig. 6. Overall element mesh

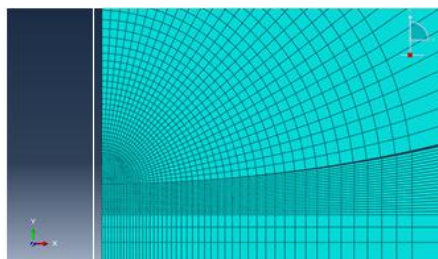
### B- Numerical Results

The finite element analysis performed in this paper has used ANSYS package to analyze the

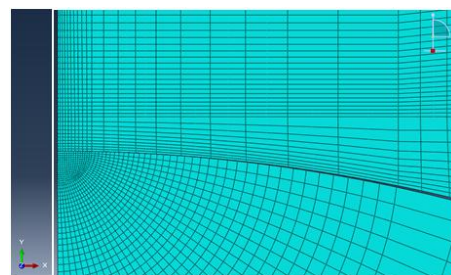
Table 1. Material properties and FEA- mesh specification

Modeling specifications								
Material properties				Element Type		Number of Elements		
E (GPa)	$S_{ut}$ (MPa)	H (Rc)	m	Linear	Quadratic	Linear	Quadratic	
210	1570	62	0.3	CAX4: A 4-node bi-quadratic axisymmetric quadrilateral.	CAX8: An 8-node bi-quadratic axisymmetric quadrilateral.	10837	10837	

Where; E=Young's modulus,  $S_{ut}$ =Ultimate strength, H= Surface hardness and m= Poison's ratio



between the ball and inner ring raceway



between the ball and outer ring raceway

Fig. 7. Element mesh at the two contact zones

## 6. DISCUSSION OF RESULTS

As mentioned before, two models of different element types are used in this numerical analysis; linear element model (CAX4) and quadratic element model (CAX8) to see which, one gives more accurate results. The results obtained from those two models have been compared with the theoretical results and showed in Figs. 8, 9 and 10 and tabulated in Table. The quadratic element model has yielded better results for the maximum contact pressures and stresses (near the theoretical results) than the Linear element. The maximum pressure has appeared on the lower half of the ball (i.e. between the ball and inner ring) with  $P_{max} = 945$  MPa which agree well with the theoretical result within an approximately deviation of 2%. Also, the maximum von-Mises stress has been found to be 592 MPa at the inner ring raceway (zone-1) as expected. The high pressure at the rolling element surface means that the ball surface may be exposed to high contact surface stress which may cause surface failure. This surface failure of the bearing may cause scuffing (as a fatigue

wear type) for the bearing. On the other hand, the high stress at the inner ring means that the stress failure may initiate from the under-surface of the inner rings causing what is called pitting (fatigue wear type) for that bearing. Therefore, the main conclusion raised here from these results of high contact pressure and high stress is explaining the main types of the two predominant failure which appear in rolling bearings: Scuffing and pitting. Therefore, to overcome these two failures, the lubrication is very important for such bearing to overcome the scuffing, simultaneously with the applied load which must be in the design recommended values to reduce the pitting of the rolling bearings.

The finite element results for pressures and stresses have been compared graphically with the analytical ones in Fig. 11 to show the validity of the proposed numerical model. The comparison showed a good agreement between them which reflects the validity of obtained results. The results also agreed well with the results obtained by reference [5 and 9].

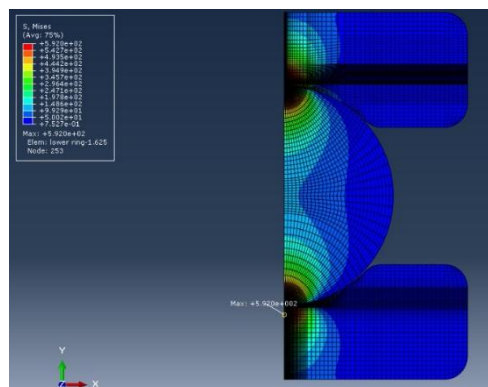
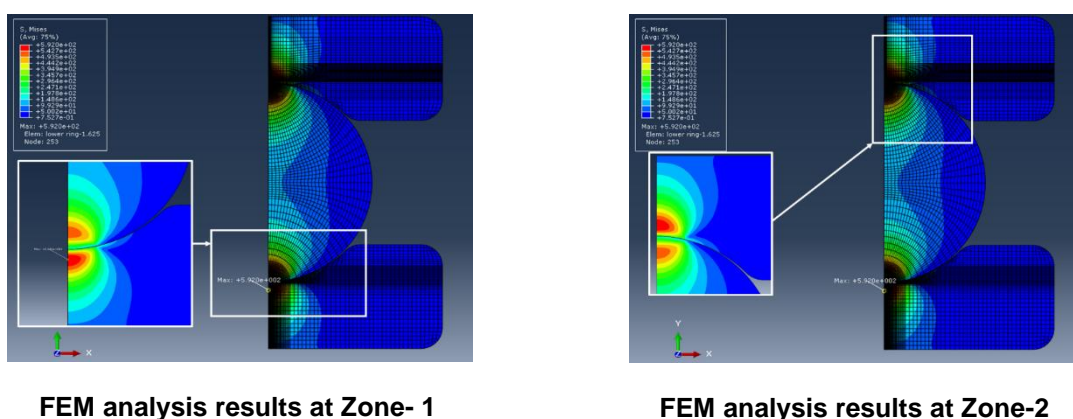


Fig. 8. FEM analysis results (equivalent von-Mises)



FEM analysis results at Zone- 1

FEM analysis results at Zone-2

Fig. 9. FEM analysis results (equivalent von-Mises)

**Table 2. Theoretical and numerical results comparison for ball bearing (Linear element-CAX4)**

Part		ZONE 1		ZONE 2		Error %			
<b>Total # of elements</b>	<b>10951</b>								
OUTPUT	Theoretical (Hertzian) contact stress data	Zone-1 Upper ball half	Outer ring raceway	Zone-2 Lower ball half	Inner ring raceway	Zone-1 Upper ball half	Outer ring raceway	Zone-2 Lower ball half	Inner ring raceway
Max. Contact pressure, P (MPa)	961.64	951.69	801.55	813.09	811.30	1.03%	16.65%	15.45%	15.63%
Max. von-Mises stress, (MPa)	596.26	493.45	530.61	494.00	550.01	17.24%	11.01%	17.15%	7.76%
Distance of the Max. stress from surface, mm	0.629	0.59	0.35	0.59	0.32	6.89%	44.24%	6.48%	49.23%

**Table 3. Theoretical and numerical result comparison for ball bearing (QUAD element-CAX8)**

Part		ZONE 1		ZONE 2		Error %			
<b>Total # of elements</b>	<b>10951</b>								
OUTPUT	Theoretical (Hertzian) contact stress data	Zone-1 Upper ball half	Outer ring raceway	Zone-2 Lower ball half	Inner ring raceway	Zone-1 Upper ball half	Outer ring raceway	Zone-2 Lower ball half	Inner ring raceway
Max. Contact pressure, P (MPa)	961.64	909.32	903.32	945.95	877.48	5.44%	6.05%	1.63%	8.75%
Max. von-Mises stress, (MPa)	596.26	524.83	591.83	523.99	592.01	11.98%	0.74%	12.12%	0.71%
Distance of Max. stress from surface	0.629	0.656	0.419	0.656	0.407	-4.22%	33.37%	-4.22%	35.27%
Max. shear stress (MPa)	298.13	262.41	295.91	261.99	296.00	11.98%	0.74%	12.12%	0.71%
Distance of Max. shear from surface	0.63	0.66	0.42	0.66	0.41	-4.22%	33.37%	-4.22%	35.27%

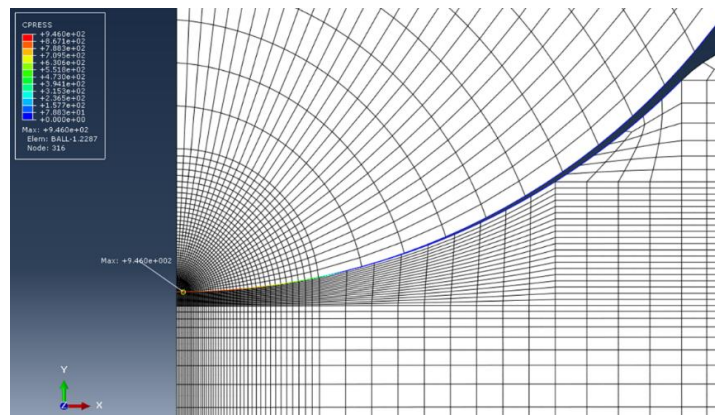


Fig. 10. FEM analysis result of the Maximum contact pressure at Zone-1

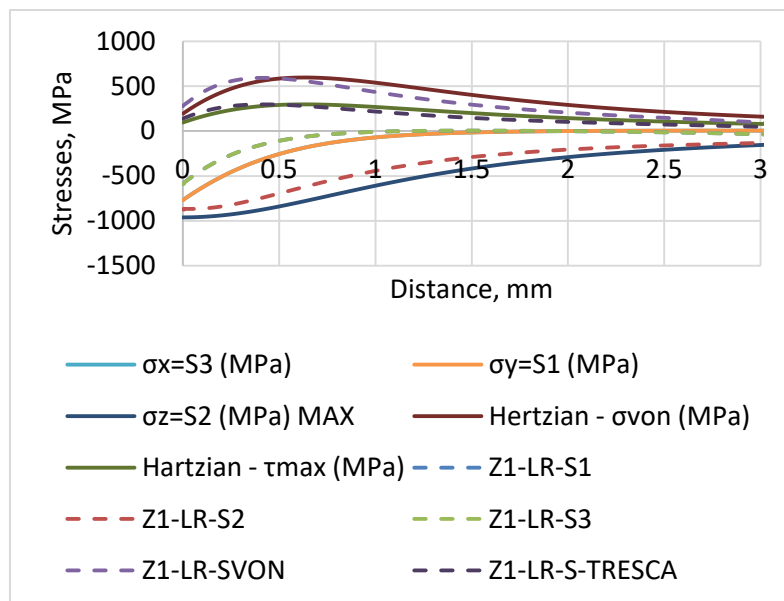


Fig. 11. Comparison between Hertzian and FEA stresses in the lower ring raceway

## 7. CONCLUSIONS

Throughout the analysis performed in this research paper, the following conclusions could be withdrawn:

- The results of the FEM stress analysis showed a good agreement with the theoretical Hertzian contact pressure and maximum equivalent von-Mises stresses.
- The maximum contact pressure was appeared on the lower half of ball with  $P_{max} = 951.69$  MPa which agree with the theoretical result within 1% deviation.
- The maximum von-Mises stress was found to be 550 MPa at the lower ring raceway (zone-1) as expected at a distance of 0.32 from surface.

- The failure in the rolling elements of bearings may be a scuffing (as fatigue wear type) due to the high contact pressure at the ball surface. Whereas, the inner rings failure may be a pitting due to the high induced stresses in the under-surface of rings.

## COMPETING INTERESTS

Authors have declared that no competing interests exist.

## REFERENCES

1. Hertz H. On the contact of elastic solids. J. Reine Angew. Math. Translated and reprinted in English in Hertz's

- Miscellaneous Papers, Macmillan & Co., London, 1896, Ch. 5. 1881;92:156–171.
2. Mootoka M, Li S. A finite element method used for contact analysis of rolling bearings. Available: <https://www.sci-en-tech.com/ICCM2017/PDFs/2199-9211-1-PB.pdf>
  3. Viramgama Parth D. Analysis of single row deep groove ball bearing”, Int. Journal of Engineering Research & Technology (IJERT), ISSN: 2278-0181. 2014;3(5).
  4. Peter Sulka, Sapietova A, Dekys V, Sapieta M. Comparison of analytical and numerical solution of bearing contact analysis. MATEC Web of Conferences. 2019;254:02022. Available: <https://doi.org/10.1051/mateconf/201925402022>, MMS 2018.
  5. Belabend S, Paunoiu V, Baroiu N, Khelif R, Iacob I. Static structural analysis analytical and numerical of ball bearings. IOP Conf. Series: Materials Science and Engineering. 2020;968. DOI: 10.1088/1757-899X/968/1/012026
  6. Tatjana L, Ristivojevic M, Mitrovic R. Mathematical model of load distribution in rolling bearing, FME Transactions 36. 2008;36(4):189-196.
  7. Richard G, Nisbett JK, Shigley E. Mechanical engineering design. McGraw-Hill Series in Mechanical Engineering, 9<sup>th</sup> Ed; 2011.
  8. ABAQUS user's manual. ABAQUS 6.12-2. Dassault systems Simulia Corp. Providence, RI, USA; 2013.
  9. Bedairi B, El-Sherbeeney A, Azzam B. Influence of mounting fits on the effective clearances and stresses in ball bearings. Int. Journal of Development Research. 2019;09(10):30862-30869.
  10. Fred BO, Zaretsky E, Poplawski J. Effect of internal clearance on load distribution and life of Radially loaded ball and roller bearings. 65th Annual Meeting and Exhibition sponsored by the Society of tribologists and lubrication engineers (STLE) Las Vegas, Nevada; 2010.
  11. Vidyasagar R, Borker B. Finite element analysis of integral shaft bearing. Int. Journal of Emerging Eng. Research and Technology. 2015;3(1):28-36. ISSN 2349-4395 (Print) & ISSN 2349-4409 (Online).

© 2021 Bedairi et al.; This is an Open Access article distributed under the terms of the Creative Commons Attribution License (<http://creativecommons.org/licenses/by/4.0>), which permits unrestricted use, distribution, and reproduction in any medium, provided the original work is properly cited.

*Peer-review history:*

*The peer review history for this paper can be accessed here:*  
<https://www.sdiarticle4.com/review-history/71436>